Journal of Alloys and Compounds 509 (2011) 2149–2153

Contents lists available at ScienceDirect

Journal of Alloys and Compounds

journal homepage: www.elsevier.com/locate/jallcom

Ferromagnetism induced by donor-related defects in Co-doped ZnO thin films

Liqiang Zhang[a], Zhizhen Ye[a], Bin Lu[a], Jianguo Lu[a,*], Yinzhu Zhang[a], Liping Zhu[a], Jingyun Huang[a], Weiguang Zhang[a], Jun Huang[a], Jun Zhang[a], Jie Jiang[a], Kewei Wu[a], Zhi Xie[b]

[a] State Key Laboratory of Silicon Materials & Department of Materials Science and Engineering, Zhejiang University, Hangzhou 310027, People's Republic of China
[b] National Synchrotron Radiation Laboratory, University of Science and Technology of China, Hefei 230029, People's Republic of China

ARTICLE INFO

Article history:
Received 25 May 2010
Received in revised form 22 October 2010
Accepted 27 October 2010
Available online 4 November 2010

PACS:
75.50.Pp
61.72.Vv
81.15.Fg

Keywords:
Diluted magnetic semiconductor
Co-doped ZnO thin film
Pulsed laser deposition

ABSTRACT

Co-monodoped ZnO (ZnCoO), Co–Ga codoped ZnO (Zn(Co,Ga)O), and Co–Na codoped ZnO (Zn(Co,Na)O) thin films were prepared on sapphire substrates by pulsed laser deposition. Their structural, optical, electrical, and magnetic properties were studied to clarify the origin of ferromagnetism (FM) in the ZnCoO system. Both the ZnCoO and Zn(Co,Ga)O films showed an n-type conductivity with a similar room-temperature ferromagnetism (RTFM), although the electron concentration of the Zn(Co,Ga)O film ($\sim 10^{21}$ cm^{-3}) was evidently higher than that of the ZnCoO film. The increasing donor density did not affect the FM greatly. The Zn(Co,Na)O film showed a p-type conductivity, but it did not show RTFM. To explore the mechanism of FM, the samples were annealed after growth. The ZnCoO and Zn(Co,Ga)O films annealed in the Ar ambient displayed similar FM features to the as-grown ones, but all of them lost their original RTFM when annealed in the O_2 ambient. The Zn(Co,Na)O film annealed in Ar exhibited a high resistivity, while a better p-type behavior than the as-grown one was observed for the Zn(Co,Na)O film annealed in O_2, however, both of them showed paramagnetism. No clusters, precipitates, or secondary phases were found from the X-ray diffraction pattern and the photoelectron K-edge X-ray absorption near-edge structure measurements. Together with the X-ray spectroscopy and photoluminescence results, it was found that the oxygen vacancy (V_o), a donor-related defect, played a vital role in determining the RTFM in the ZnCoO system.

Published by Elsevier B.V.

1. Introduction

Diluted magnetic semiconductors (DMSs) have attracted increasing attention because of their potential for spintronics [1]. The main challenge in DMS materials is to obtain the intrinsic ferromagnetism (FM) with Curie temperature above room temperature (RT). Dietl et al. [2] theoretically predicted the ferromagnetism with a very high Curie temperature in p-type $Zn_{1-x}Mn_xO$. Since then, many efforts have been made for ZnO thin films and nanostructure materials by doping a variety of transition metals [3–9], but the origin of the room temperature ferromagnetism (RTFM) is still a controversial issue and it has been explained from the point of either microstructural details [10] or dopant defects [11]. The reproducibility and the origin of the RTFM are still great challenges. Sato and Katayama-Yoshida [12] showed that the RTFM appeared in n-type ZnCoO. However, Spaldin [13] and Jayakumar et al. [14] argued that the hole doping could enhance the ferromagnetism in ZnCoO. Recently, researchers reclaimed that the donors are the key factor in determining the RTFM in fact [15–17]. For instance, Zn interstitials (Zn_i) were the cause of RTFM in ZnCoO [15,16]. Nevertheless, it was calculated that the oxygen vacancies (V_o) are the medium of the long distance ferromagnetic interaction between the Co^{2+} ions as well [17].

In order to clarify the relationship between the carrier, intrinsic defect, and the RTFM, Co-monodoped ZnO (ZnCoO), Co–Ga codoped ZnO (Zn(Co,Ga)O), and Co–Na codoped ZnO (Zn(Co,Na)O) thin films were fabricated on sapphire substrates by pulsed laser deposition (PLD). All the samples were post-annealed in an Ar or O_2 environment after the film fabrication to explore the FM mechanism. The as-grown ZnCoO thin films were n-type due to the intrinsic Zn_i and V_o defects. In our previous studies, the Na dopant showed good potential to realize p-type conversion in ZnO [18,19], and the Ga doping could enhance the n-type carrier density of ZnO [20]. Thus, in this study we introduced the Na and Ga into ZnCoO films to study the p- and n-type conductivities in ZnCoO and their influence on the RTFM. The structural, optical, electrical, and magnetic properties of the films were investigated in detail to make clear the origin of RTFM in the ZnCoO system.

2. Experimental

ZnCoO, Zn(Co,Ga)O, and Zn(Co,Na)O thin films were prepared on *c*-plane (0 0 0 1) single crystal sapphire substrates by PLD. The ceramic targets were prepared by mixing ZnO, Co_2O_3, Ga_2O_3, and/or Na_2CO_3 powders. In the ZnCoO target, the Co content was 5 at.%; in the Zn(Co,Ga)O target, the Co content was 5 at.% and Ga was 1 at.%; in the Zn(Co,Na)O target, the Co content was 5 at.% and Na was 1 at.%, respectively. A

* Corresponding author. Tel.: +86 571 8795 2187; fax: +86 571 8795 2625.
E-mail address: lujianguo@zju.edu.cn (J. Lu).

0925-8388/$ – see front matter. Published by Elsevier B.V.
doi:10.1016/j.jallcom.2010.10.171

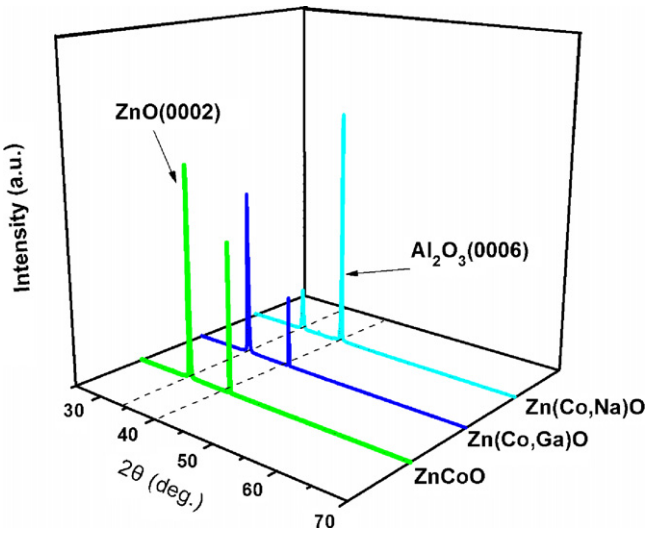

Fig. 1. (Color online) XRD patterns of the as-grown ZnCoO, Zn(Co,Ga)O, and Zn(Co,Na)O films deposited on (0 0 0 1) sapphire substrates.

KrF excimer laser (Compex102, 248 nm, 25 ns) was used as the ablation source. The chamber was evacuated to a base pressure of 4×10^{-4} Pa and then high-purity O_2 (99.999%) was introduced as the ambient gas with the working pressure of 0.02 Pa. The substrates were held at 400 °C during growth. All the films were grown for 30 min with the thicknesses of about 500 nm. After the film fabrication, the samples were post-annealed at 500 °C for 30 min in the Ar (40 Pa) and O_2 (40 Pa) ambient, respectively.

The film structure and crystalline quality were characterized by a Bede D1 X-ray diffraction (XRD) system with a Cu Kα source (λ = 0.15406 nm). The electrical properties were investigated by a four-point probe van der Pauw configuration (HL5500PC) at RT. Field-emission scanning electron microscope (FE-SEM) was used to study the morphologies of the films. The transmittance spectra of films were investigated in the wavelength range from 300 to 800 nm by a Varian Cary-300 spectrophotometer. To determine the valence state and local geometry of the Co dopant in the host ZnO lattice, the Co K-edge X-ray absorption near-edge structure (XANES) measurements were carried out. Magnetization studies were performed using the superconducting quantum interference device (SQUID) magnetometer. X-ray photoelectron spectroscopy (XPS) and photoluminescence (PL) measurements were done to study the oxygen defect density. Additionally, the induced-coupled-plasma (ICP) atomic emission spectrum was used to determine the Co contents in samples after measuring their magnetic properties.

3. Results and discussion

Fig. 1 shows the XRD patterns of the as-grown ZnCoO, Zn(Co,Ga)O, and Zn(Co,Na)O films. All the films are highly (0 0 0 2) preferred oriented without additional peaks, suggesting that no secondary phases such as Co_2O_3 were found within the sensitivity of XRD measurements. As the size of the major dopant Co^{2+} (0.58 Å) is close to that of Zn^{2+} (0.60 Å) and the amount of Na^+ and Ga^{3+} dopants is small, the (0 0 0 2) peak positions are very similar to that of the standard ZnO powders ($2\theta = 34.45°$).

Table 1 lists the electrical properties (e.g., resistivity (ρ), mobility (μ), and carrier concentration (n)) of the as-grown and post-annealed samples. The as-grown ZnCoO and Zn(Co,Ga)O films were n-type with the electron concentrations of 4.51×10^{18} cm^{-3} and 1.10×10^{21} cm^{-3}, respectively. The as-grown Zn(Co,Na)O film displayed p-type conductibility with the hole concentration of $\sim 10^{16}$ cm^{-3}. The introduction of Ga atoms into ZnCoO films can improve the n-type conduction, as that previously reported in Ga-doped ZnO [21], while the Na doping realizes the p-type conversion, which is consistent with the theoretical predication [22] and experimental confirmation in ZnO [18,19]. The introduced Ga acts as a donor to realize the n-type enhancement and the doped Na acts as an acceptor to make the p-type conversion. The codoping method may be an effective way to fabricate the p-type ZnO [23]. The conversion from n-type to p-type contributes to the study of the influence of carrier on the RTFM of the ZnCoO system. It is worth noting that the resistivity of ZnCoO film increases from 0.030 Ω cm when annealed in Ar to 27.15 Ω cm when annealed in O_2, indicating a change in defect concentration. Another interesting finding is that the Zn(Co,Na)O film reveals a p-type conductivity with a higher hole concentration of $\sim 10^{18}$ cm^{-3} after being annealed in O_2, which needs to be further studied.

Fig. 2(a)–(C) shows the surface morphologies of ZnCoO, Zn(Co,Ga)O, and Zn(Co,Na)O films. All the films display relatively smooth surface and close-packed grains. No obvious voids and defects over the films are observed, which indicates that the films are of acceptable crystallinity.

The optical transmittance spectra of ZnCoO, Zn(Co,Ga)O, and Zn(Co,Na)O films in the wavelength from 300 to 800 nm are presented in Fig. 3(a). In the spectra, three absorption bands, located at approximately 569, 613, and 662 nm, respectively, are found in all the cases, regardless of the doping methods. The three peaks are the characteristic ones in ZnCoO thin film, attributed to the typical d–d transitions: $^4A_2(F) \rightarrow {}^2A_1(G)$, $^4A_2(F) \rightarrow {}^4T_1(P)$, and $^4A_2(F) \rightarrow {}^2E(G)$, respectively. The d–d transitions come from the Co^{2+} in place of Zn^{2+} [24].

Fig. 3(b) shows the variation of the optical band gap (E_g) of ZnCoO, Zn(Co,Ga)O, and Zn(Co,Na)O thin films. The absorption coefficient (α) can be calculated by the Lambert formula, $\alpha = [\ln(1/T_r)]/t$, where T_r is the transmittance and t is the thickness. From the $(\alpha h\nu)^2$ versus $h\nu$ (Tauc relation) plot, the band gap energies can be obtained by the extrapolation of the linear region to $\alpha = 0$ [25]. The E_g values are determined to be 3.18, 3.40, 3.48 eV for the Zn(Co,Na)O, ZnCoO, and Zn(Co,Ga)O films, respectively. The band-gap narrowing of the Zn(Co,Na)O film, as compared with that of the ZnCoO film, may be due to the merging of the impurity band with the valance band, which was commonly observed in p-type ZnO [26]. As the electron concentration of the Zn(Co,Ga)O film increases greatly with the Ga doping and is up to 10^{21} cm^{-3}, the band gap is broadened due to the Burstein–Moss (B–M) shift effect [27].

In order to obtain the valence state and local geometry of the Co dopant in films, the Co K-edge XANES was employed, as shown

Table 1
Resistivity (ρ), mobility (μ), and carrier concentration (n) of the as-grown and annealed ZnCoO, Zn(Co,Ga)O, and Zn(Co,Na)O films.

Sample	Condition	μ (cm^2 V^{-1} S^{-1})	ρ (Ω cm)	N (cm^{-3})	Type
ZnCoO	As-grown	4.44	0.313	4.51×10^{18}	n
	Annealed in Ar	5.16	0.030	4.01×10^{19}	n
	Annealed in O_2	0.0968	27.15	2.37×10^{18}	n
Zn(Co,Ga)O	As-grown	5.39	0.0011	1.10×10^{21}	n
	Annealed in Ar	10.9	0.0086	6.67×10^{19}	n
	Annealed in O_2	31.4	0.0043	4.61×10^{19}	n
Zn(Co,Na)O	As-grown	0.364	626.2	2.74×10^{16}	p
	Annealed in Ar	–	–	–	–
	Annealed in O_2	0.323	15.24	1.27×10^{18}	p

"–" Means that it is out of the range of Hall-effect measurements.

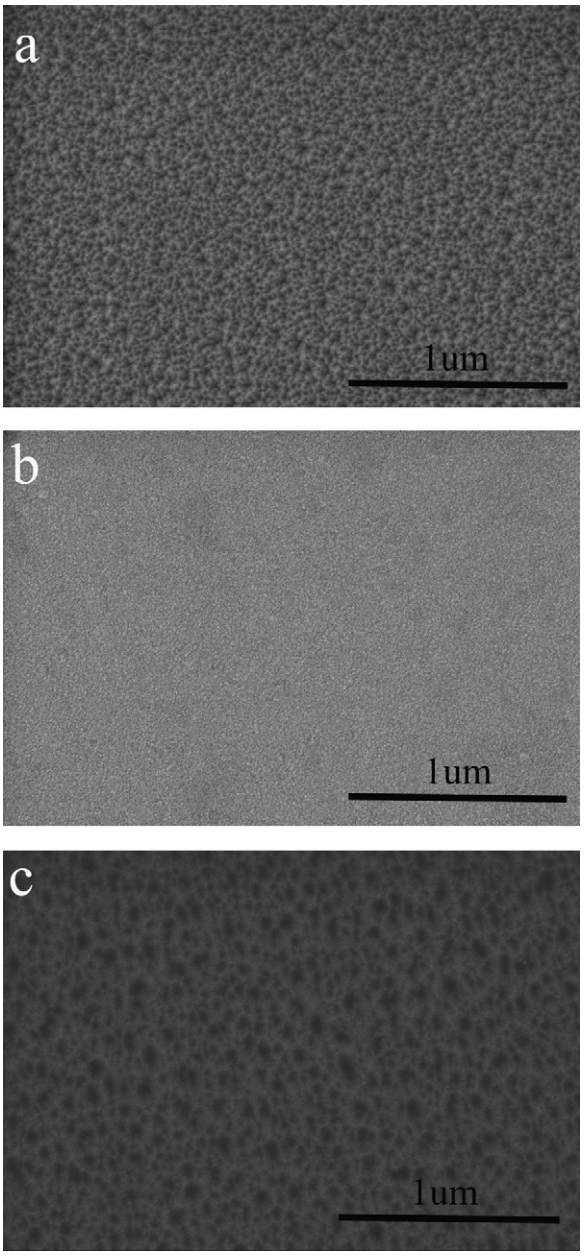

Fig. 2. SEM images of the as-grown ZnCoO (a), Zn(Co,Ga)O (b), and Zn(Co,Na)O (c) films on sapphire substrates by PLD.

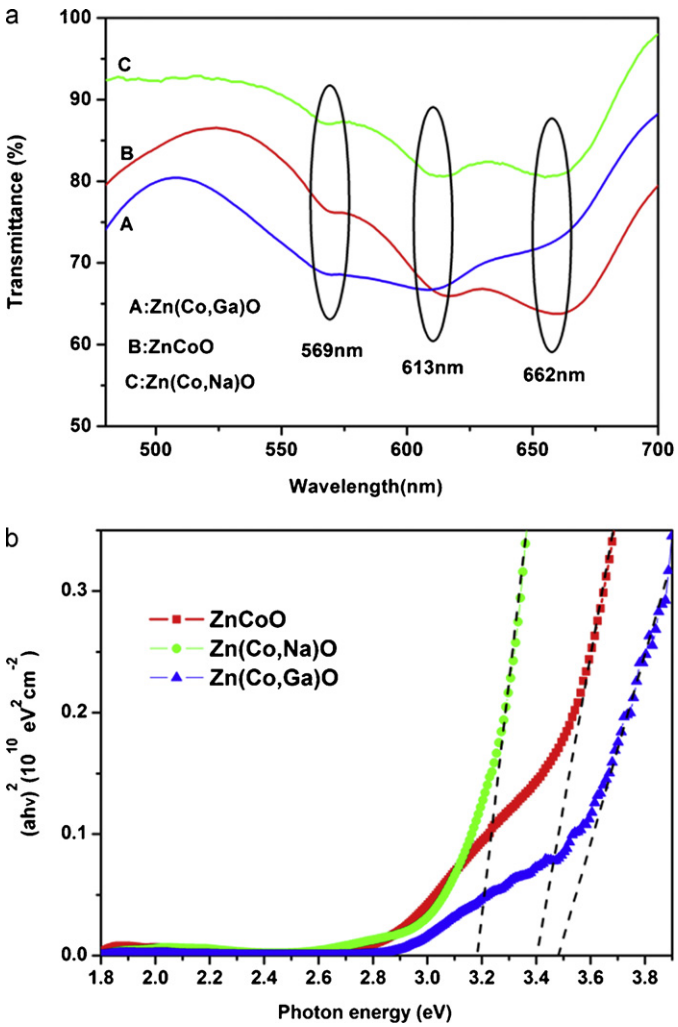

Fig. 3. (Color online) (a) Transmittance spectra of the as-grown ZnCoO, Zn(Co,Ga)O, and Zn(Co,Na)O thin films. (b) Optical bandgap plots of ZnCoO, Zn(Co,Ga)O, and Zn(Co,Na)O thin films.

in Fig. 4. The Co K-edge XANES has the advantage of sensitivity to the chemical shift between the onset of absorption for Co^0 and Co^{2+}, which can provide the information of the existing forms of Co in the lattice. From the spectra, obvious discrepancy among them was found, indicating that the Co^{2+} was in the position of Zn^{2+}, instead of forming metal Co, Co_2O_3, or CoO clusters. Thus, it is now safe to conclude that the Co^{2+} systematically substitutes Zn^{2+} in the lattice, as claimed in other literatures [11,28,29]. The possibility of existence of Co metal cluster or formation of secondary phases such as CoO and Co_2O_3 can be excluded.

Fig. 5 shows the magnetization of the ZnCoO, Zn(Co,Ga)O, and Zn(Co,Na)O thin films. Magnetic measurements were carried out using SQUID magnetometer at RT. The magnetic field was applied parallel to the film plane, and the background signals were subtracted. The actual cobalt number was determined by the ICP atomic emission spectra. The ZnCoO and Zn(Co,Ga)O thin films show the obvious hysteresis loops at RT. The value of the satu-

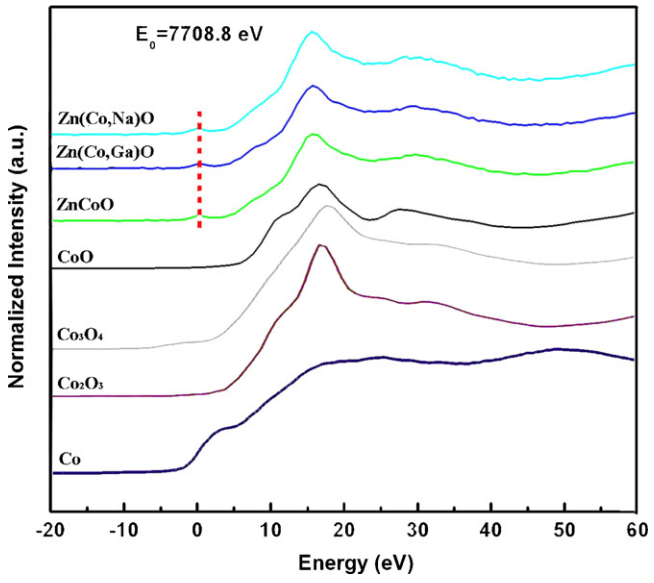

Fig. 4. (Color online) Co K-edge XANES spectra for different specimens: metal Co, Co_2O_3, Co_3O_4, CoO, ZnCoO, Zn(Co,Ga)O, and Zn(Co,Na)O thin film. The threshold energy E_0 of Co = 7708.8 eV is for reference.

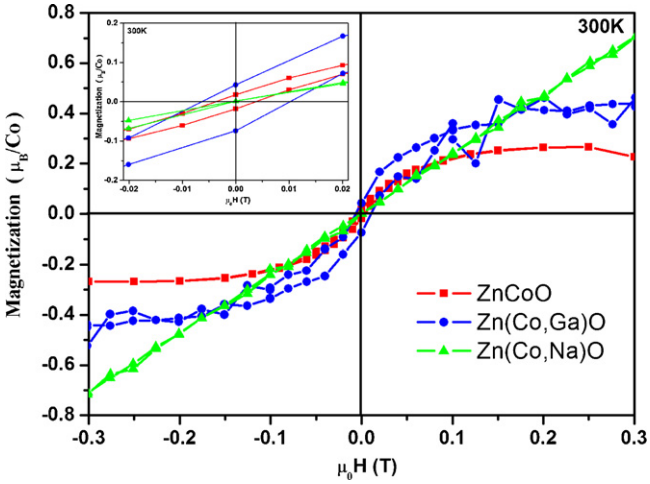

Fig. 5. (Color online) Magnetization of the as-grown ZnCoO, Zn(Co,Ga)O, and Zn(Co,Na)O thin films at RT. The inset shows the magnetization of the films in a magnified scale.

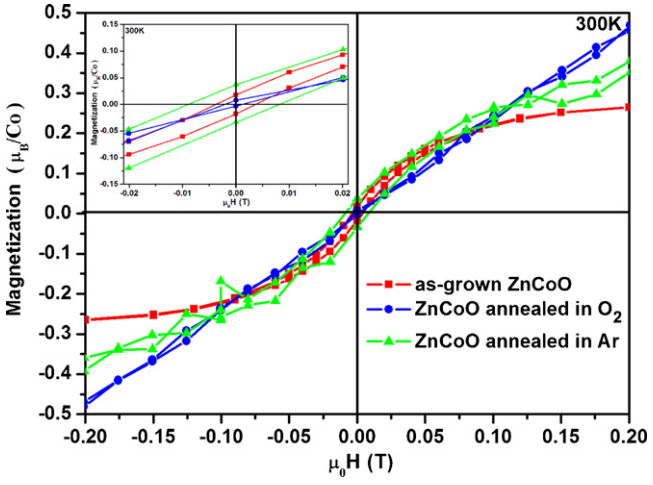

Fig. 6. (Color online) Magnetization of the as grown ZnCoO thin film, the ZnCoO thin films annealed in Ar, and the ZnCoO thin film annealed in O_2. The inset shows the magnetization of the films in a magnified scale.

ration magnetization (Ms) for the Zn(Co,Ga)O film is 0.42 μB/Co, which is higher than that of the ZnCoO film (0.27 μB/Co). The Zn(Co,Na)O film fabricated at the same condition shows a paramagnetism behavior. The introduction of Ga greatly enhances the electron density of the films, which, however, does not affect the RTFM evidently. It seems that a high content of introduced donors is not the key contributor to forming the FM in the ZnCoO film, but an n-type environment in ZnCoO is crucial to realize the FM. Also, it is indicated that the high electron density is not the key reason for the formation of RTFM. Since the isolated Co^{2+} ions have a short-range magnetic interaction, the RTFM of the ZnCoO and Zn(Co,Ga)O films can only be realized by the certain substance behaving as a long-range Coulomb interaction medium [30]. The most intrinsic defects in ZnO are Zn_i and V_o. Recently the theoretical modeling revealed that the Co^{2+}–V_o pair interaction was the origin of the FM [12]. Pan et al. [31] also reported that the RTFM came from the Co–V_o and Co–Zn_i pairs, which acted as the magnetic centers for the long-range magnetic coupling.

To test the hypothesis that the donor-related defect of V_o is crucial to the RTFM, all the samples were annealed in the Ar and O_2 environment to obtain their different oxygen defect densities. The magnetization results of the ZnCoO and Zn(Co,Ga)O films annealed in both Ar and O_2 were similar. Here, we just discuss the magnetization of the ZnCoO thin film as an example and the result is shown in Fig. 6. The RTFM of ZnCoO films is due to the hybridization of Co ion states and the charge carrier introduced by shallow donors at the Fermi level [32]. The most common shallow donors in ZnO are the Zn_i and V_o. There existed a large amount of V_o for the ZnCoO film grown in the O_2 environment at a low pressure. Annealing in an O_2 environment at a high pressure could reduce the density of V_o greatly, and as a result, the ZnCoO thin film lost its original RTFM. The annealing in an Ar environment cannot enhance the V_o density greatly of the ZnCoO film, as well as the Ms of the RTFM. It is suggested that the V_o plays a crucial role in realizing the RTFM. Fonin et al. [33] also found that the oxygen vacancies or oxygen related defects, rather than the zinc related defects, constituted the bound magnetic polarons. The Zn(Co,Na)O film showed a high resistance after annealling in Ar and a good p-type behavior when annealed in O_2, but both of them showed paramagnetism. The observation indicates that the Co–Na codoping method may be an appropriate choice to realize the p-type conversion, but it was detrimental to the RTFM of ZnCoO.

Fig. 7 shows the O 1*s* core level spectra of the as-grown ZnCoO film and the annealed ZnCoO films in the Ar and O_2 ambients. The O 1*s* XPS results showed a clear evidence of the variation of the oxygen defect densities before and after annealing. The lowest peak in binding energy located at 529.9 ± 0.3 eV (red line) is attributed to the intrinsic O^{2-} ions in the wurtzite structure of the hexagonal Zn^{2+} ion array [34]; the middle one located at 531.5 ± 0.3 eV (green line) is attributed to the O^{2-} ions that are in the oxygen deficient regions of ZnCoO; the higher one located at 532.4 ± 0.3 eV (blue line) is due to the surface influence such as H_2O and other contaminations [35,36]. The oxygen defect related peaks in the as-grown ZnCoO film and the ZnCoO film annealed in Ar are similar, which are higher than that in the ZnCoO film annealed in O_2. It indicates that there are more oxygen defects in the as-grown ZnCoO film and the ZnCoO film annealed in the Ar ambient.

In order to further confirm that there are different defect densities among the as-grown and annealed ZnCoO films, a PL study was done, as shown in Fig. 8. The broad peaks around 500 nm are due to the transitions involving deep levels in the band gap related to oxygen vacancies [37,38]. The ZnCoO film is grown in a low-oxygen-pressure (0.02 Pa) ambient and the matrix is not in stoichiometry, which leads to the broad defect band [39]. This peak experiences a sharp decrease when the ZnCoO film annealed in an oxygen rich ambient, while it is still obvious for the ZnCoO film annealed in an

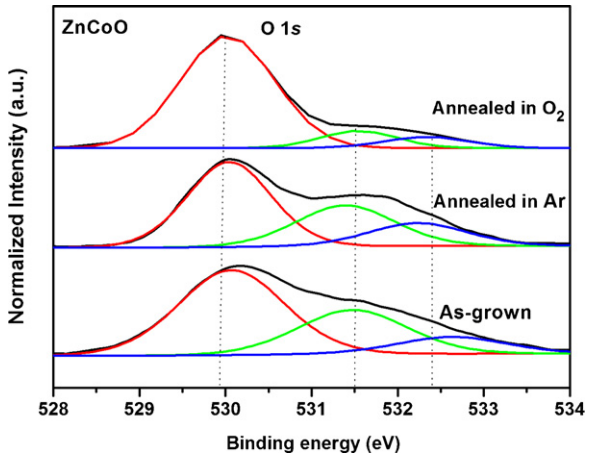

Fig. 7. (Color online) Typical O 1*s* core-level spectra (black line: experimental; red line: the fitted curve related to oxygen in the ZnO wurtzite structure; green line: the fitted curve related to defect; blue line: the fitted curve related to oxygen on the surface) for the as-grown and annealed ZnCoO thin films. The fitted peaks with various derivations are marked. For details see text.

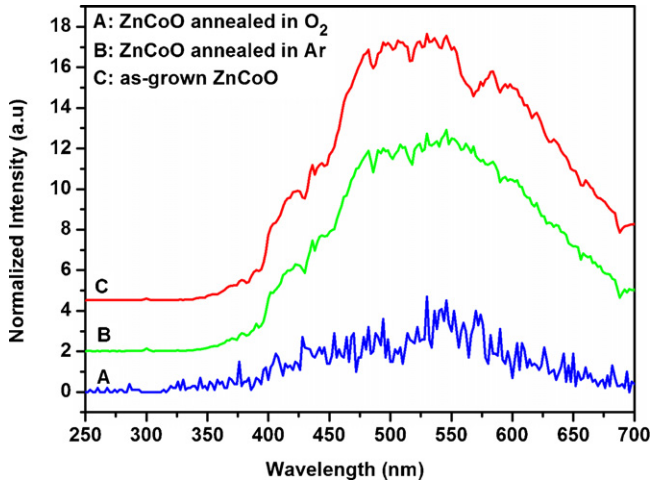

Fig. 8. Room-temperature PL spectra for the as-grown and annealed ZnCoO thin films.

Ar ambient. The results further indicate that the V_o density is different among the samples, which is corresponding to the observed RTFM in the ZnCoO system.

4. Conclusions

In summary, ZnCoO, Zn(Co,Ga)O, and Zn(Co,Na)O thin films were prepared on *c*-plane (0 0 0 1) single crystal sapphire substrates by PLD. There were not detectable secondary phases based on the results of XRD and XANES spectra. The optical absorption peaks and XANES spectra both showed that the Co^{2+} substituted Zn^{2+} in ZnCoO films. It was demonstrated that the oxygen vacancy donors in an n-type environment was the key factor to realize the RTFM in the ZnCoO system. The Co-Na codoping method was detrimental to the RTFM, although it could result in an acceptable p-type behavior in ZnCoO. The enhanced electron density in the ZnCoO film by the Ga doping seemed to be little helpful to improve the magnetization. The annealing in a high-pressure O_2 ambient was certainly detrimental to the RTFM of the ZnCoO system. Our findings indicated that the RTFM properties of ZnCoO was strongly related to the presence of oxygen vacancy defects in the host material.

Acknowledgements

This work was supported by Qianjiang Talent Project of Zhejiang Province under Grant No. 2009R10046 and National Basic Research Program of China under Grant No. 2006CB604906. The authors thank the support from the National Synchrotron Radiation Laboratory, University of Science and Technology of China and Prof. H.P. He at the City University of Hong Kong for his helpful discussions.

References

[1] J.M.D. Coey, M. Venkatesan, C.B. Fitzgerald, Nat. Mater. 4 (2005) 173.
[2] T. Dietl, H. Ohno, F. Matsukura, J. Cibert, D. Ferrand, Science 287 (2000) 1019.
[3] A. Singhal, J. Alloys Compd. 507 (2010) 312.
[4] M.M. Selim, N.M. Deraz, O.I. Elshafey, A.A. El-Asmy, J. Alloys Compd. 506 (2010) 541.
[5] L.H. Van, M.H. Hong, J. Ding, J. Alloys Compd. 449 (2008) 207.
[6] Z.L. Lu, W. Miao, W.Q. Zou, M.X. Xu, F.M. Zhang, J. Alloys Compd. 494 (2010) 392.
[7] J.J. Gu, L.H. Liu, H.T. Li, Q. Xu, H.Y. Sun, J. Alloys Compd. 508 (2010) 516.
[8] D. Paul Joseph, S. Ayyappan, C. Venkateswaran, J. Alloys Compd. 415 (2006) 225.
[9] R.K. Singhal, Arvind Samariya, Y.T. Xing, Sudhish Kumar, S.N. Dolia, U.P. Deshpande, T. Shripathi, Elisa B. Saitovitch, J. Alloys Compd. 496 (2010) 324.
[10] Y. Wang, L. Sun, L. Kong, J. Kang, X. Zhang, R. Han, J. Alloys Compd. 423 (2006) 256.
[11] C. Song, S.N. Pan, X.J. Liu, X.W. Li, F. Zeng, W.S. Yan, B. He, F. Pan, J. Phys.: Condens. Matter 19 (2007) 176229.
[12] K. Sato, H. Katayama-Yoshida, Phys. Status Solidi B 229 (2002) 673.
[13] N.A. Spaldin, Phys. Rev. B 69 (2004) 125201.
[14] O.D. Jayakumar, I.K. Gopalakrishnan, S.K. Kulshreshtha, Adv. Mater. 18 (2006) 1857.
[15] N. Khare, J. Menno, M. Kapper, Mark G. Wei, Judith L. Blamire, MacManus-Driscoll, Adv. Mater. 18 (2006) 1449.
[16] A. Dana, Schwartz, R. Daniel, Gamelin, Adv. Mater. 16 (2004) 23.
[17] C.D. Pemmaraju, R. Hanafin, T. Archer, H.B. Braun, S. Sanvitoo, Phys. Rev. B 78 (2008) 054428.
[18] Z.Z. Ye, L.Q. Zhang, J.Y. Huang, Y.Z. Zhang, L.P. Zhu, B. Lu, J.G. Lu, L. Wang, Y.Z. Jin, J. Jiang, Y. Xue, J. Zhang, S.S. Lin, D. Yang, J. Semicond. 30 (2009) 081001.
[19] L. Yang, Z.Z. Ye, L.P. Zhu, Y.J. Zeng, Y.F. Lu, B.H. Zhao, J. Electron. Mater. 36 (2007) 498.
[20] T. Prasada Rao, M.C. Santhosh Kumar, J. Alloys Compd. 506 (2010) 788.
[21] L.P. Zhu, Z.G. Ye, X.T. Wang, Z.Z. Ye, B.H. Zhao, Thin Solid Films 518 (2010) 1879.
[22] C.H. Park, S.B. Zhang, S.H. Wei, Phys. Rev. B 66 (2002) 073202.
[23] J.G. Lu, Z.Z. Ye, F. Zhuge, Y.J. Zeng, B.H. Zhao, L.P. Zhu, Appl. Phys. Lett. 85 (2004) 3134.
[24] K.J. Kim, Y.R. Park, Appl. Phys. Lett. 81 (2002) 1420.
[25] D. Paul Joseph, M. Saravanan, B. Muthuraaman, P. Renugambal, S. Sambasivam, S. Philip Raja, P. Maruthamuthu, C. Venkateswaran, Nanotechnology 19 (2008) 485707.
[26] Y.F. Yan, J.B. Li, S.H. Wei, M.M. Al-Jassim, Phys. Rev. Lett. 98 (2007) 135506.
[27] T.S. Moss, Proc. Phys. Soc. Lond. Ser. B 67 (1954) 775.
[28] K.A. Griffin, A.B. Pakhomov, C.M. Wang, S.M. Heald, Kannan M. Krishnan, Phys. Rev. Lett. 94 (2005) 157204.
[29] T.F. Shi, S.Y. Zhu, Z.H. Sun, S.Q. Wei, W.H. Liu, Appl. Phys. Lett. 90 (2007) 102108.
[30] K. Samanta, P. Bhattacharya, J.G.S. Duque, W. Iwamoto, C. Rettori, P.G. Pagliuso, R.S. Katiyar, Solid State Commun. 147 (2008) 305.
[31] F. Pan, C. Song, X.J. Liu, Y.C. Yang, F. Zeng, Mater. Sci. Eng. R 62 (2008) 1.
[32] K.R. Kittilstved, W.K. Liu, D.R. Gamelin, Nat. Mater. 59 (2006) 291.
[33] M. Fonin, G. Mayer, E. Biegger, J. Phys.: Conf. Ser. 100 (2008) 042034.
[34] G.H. Kim, D.L. Kim, B.D. Ahn, S.Y. Lee, H.J. Kim, Microelectron. J. 40 (2009) 272.
[35] M.N. Islam, T.B. Ghosh, K.L. Chopra, H.N. Acharya, Thin Solid Films 280 (1996) 20.
[36] L.Q. Zhang, Z.Z. Ye, J.G. Lu, B. Lu, Y.Z. Zhang, L.P. Zhu, J. Zhang, D. Yang, K.W. Wu, J. Huang, Z. Xie, J. Phys. D: Appl. Phys. 43 (2010) 015001.
[37] S.A. Sudenikin, M. Cocivera, J. Appl. Phys. 91 (2002) 5060.
[38] H.S. Kang, J.S. Kang, J.W. Kim, S.Y. Lee, J. Appl. Phys. 95 (2004) 1246.
[39] M. Ivill, S.J. Pearton, S. Rawal, L. Leu, P. Sadik, R. Das, A.F. Hebard, M. Chisholm, J.D. Budai, D.P. Norton, New. J. Phys. 10 (2008) 065002.